X-Band Multi-Frequency 30% Compound SCALN Microacustic Resonators and Filters for 5G-Advanced and 6G Applications

Gabriel Giribaldi, Michele Pirro, Meruyert Assylbekova, Bernard Herrera, Giuseppe Michetti, Luca Colombo, and Matteo Rinaldi

Northeastern SMART Center, Northeastern University, Boston, USA

Summary-This paper reports on record-high resonance frequency-quality factor product ($f_s \cdot Q$) figure of merit 30% Sc-doped Aluminum Nitride (ScAlN) Cross-sectional Lamé Mode (CLM) microacustic resonators in the super high frequency (SHF) range, along with outstanding electromechanical coupling-quality factor products ($k_t^2 \cdot Q$). Moreover, for the first time above 5 GHz, ScAlN-based resonators have been arranged to produce first-order passband ladder filters, providing record-wide fractional bandwidth for the microacoustic technology in the same frequency range. The ScAlN piezoelectric material was deposited from a compound casted target on a 200 mm wafer, going into the direction of a foundry-standardized fabrication process for SHF resonators. This first-of-a-kind demonstration paves the way for the synthesis of high-performance commercial filters for communication in the 5G era and beyond, where SHF operation and wide carrier bandwidth are fundamental requirements.

I. INTRODUCTION

The introduction of the 5th generation mobile networks (5G) has enabled wireless communication with unprecedented data-rate, spectral efficiency, and latency [1]. Vehicle-to-vehicle and vehicle-to-infrastructure communication, massive Internet of Things (IoT) networks, highly-immersive virtual reality, and development of the Metaverse itself are just few examples of the possible technological innovation that are, or can be, made possible by an advancement in the data communication paradigm. Such a leap comes with several technological challenges associated with the hardware required for filtering components. Key enablers in 4G and older generations, such as Surface Acoustic Wave (SAW) resonators for sub-GHz frequencies and thin-Film Bulk Acoustic Resonators (FBARs) for GHz-range bands suffer either from difficult scalability above 10 GHz, or difficult on-chip tuning of the resonance frequency, resulting in an unacceptable level of losses for the filters or a costly and time-consuming fabrication process. Therefore, they must be substituted by more versatile, efficient, and simpler to fabricate and integrate designs. While the sub-6 GHz frequency range has already been commercialized still taking advantage of the Aluminum Nitride (AlN) or lightly doped ScAlN FBARs, the mm-Wave spectrum is open to new solutions [2][3]. From a material standpoint, the recent discovery of Scandium (Sc) doping of AlN has proven to dramatically improve its piezoelectric coefficients [4]. In particular, given their quadratic or cubic dependence with the dopant concentration, high doping levels (Sc[%] $\geq$ 30%) provide the highest degree of improvement in the film piezoelectric response. Such a material properties enhancement directly translates in devices able to attain much higher values of electromechanical coupling (k_t^2) [5], which in turn is closely linked to the bandwidth of microacoustic filters implementing resonators as building blocks. Therefore, the ScAlN technology has the potentiality of enabling the fabrication of devices with performance well beyond the state-of-the-art to become the building blocks for passive pass-band filters in RadioFrequency front ends (RFFE).

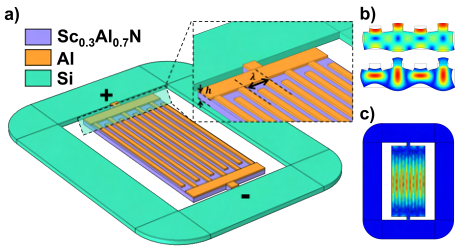

Figure 1: a) 3D view of a LFE CLMR. The + and - terminals, along with the materials and key geometrical dimensions are highlighted, b) displacement and stress profile in a 2D cross-section of the device, showing the Cross-sectional Lamé modeshape, and c) 3D top view of the displacement of a LFE CLMR at resonance. The 2D and 3D plots of b) and c) have been obtained via COMSOL® Multiphysics Finite element modeling simulations.

The recently demonstrated Cross-sectional Lamé Mode resonators (CLMRs) [6], given their reliance on a 2-dimensional mode of vibration, proved to be a competitive technology both in terms of k_t^2 and quality factor (Q). While the first directly translates to the maximum achievable filter bandwidth, the latter has an impact on the insertion loss and the filter selectivity. What is more appealing in CLMRs, is their on-chip frequency tunability. In fact, just by lithographically adjusting their horizontal acoustic wavelength (λ) it is possible to sweep the operating frequency over a broad range without major k_t^2 degradation. Among the possible CLMR topologies [5], the lateral field-excited (LFE) configuration (Fig.1), though exhibiting degraded k_t^2 compared to designs relying on a more vertical excitation, can be fabricated with an extremely simple (ideally 2 masks) micro-machining process. Moreover, given the lower mass-loading of the electrodes, LFE is the topology that allows to reach the highest resonance frequency (f_s) per same λ, thus relaxing the lithographic constraint on the electrode in-plane dimensions. While SHF ScAlN microacustic resonators

have been already presented [7][8], this work leverages the sputter deposition of high-quality piezoelectric ScAlN thin-films with high doping level to fabricate devices with unprecedented and ground-breaking performance figures of merit (FoM). Moreover, to the authors' knowledge, for the first time above 5 GHz, ScAlN and/or CLMR devices have been arranged into first-order ladder filters, providing wide fractional bandwidth. Combining these advantages with ScAlN post-CMOS compatibility, this work hints to the possible mass-production of high-performing devices for the next generation of RFFE communication filters for 5G-advanced and 6G applications [9]. For the first time, highly doped ScAlN emerges as solid commercial competitor to AlN in the framework of passive RF filtering devices, with high innovation capabilities.

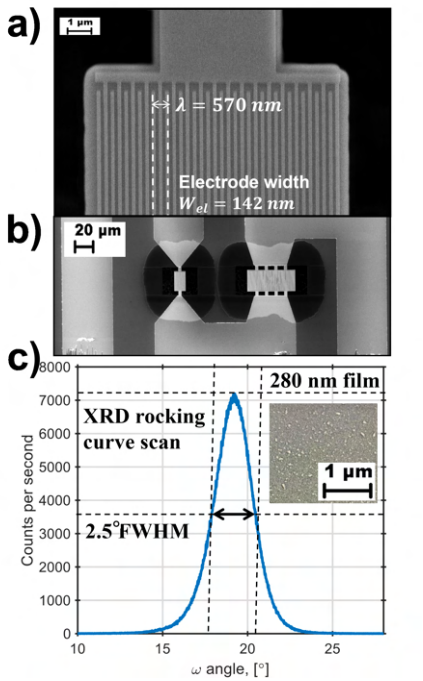

Figure 2: Scanning Electron Microscope (SEM) top view pictures of devices fabricated in this work, respectively (a) a standalone resonator and (b) a ladder filter, with highlighted the relevant dimensions and c) X-ray diffractometry (XRD) rocking curve scan of the $Sc_{0.3}Al_{0.7}N$ 280 nm layer. The optimized Full Width Half Maximum of 2.5° is highlighted, while the inset shows a SEM top view picture, revealing the low count of abnormally oriented grains.

II. METHODOLOGY

Fabrication

$Sc_{0.3}Al_{0.7}N$ multi-frequency LFE CLMR standalone resonators and first-order ladder filters were fabricated (Fig.2a-b) with an extremely simple micro-machining process. First, a 280 nm 30% ScAlN film was deposited via reactive sputtering on a 200 mm high-resistivity Si<100> wafer. The deposition exploited a 12" AlSc compound casted target and an industrial-grade EVATEC Clusterline tool. The film high quality was obtained through an optimization process targeting low in-plane stress ($< \pm 200$ MPa), high uniformity (roughness $R < 2$ nm), high throughput (depostion rate 44.2 nm/min), low abnormally oriented grains (AoGs) count, and low Full Width Half Maximum (FWHM $= 2.5°$, Fig.2c). Afterwards, the piezoelectric layer was etched via Reactive Ion Etching (RIE) utilizing a recipe with high power, high Argon concentration and chlorine chemistry. To improve the final resonant plate sidewall (SW $> 70°$), a SiO_2 hard mask was employed. It was deposited by plasma-enhanced chemical vapor deposition (PECVD), dry-etched in fluorine chemistry, and stripped in 49% hydrofluoric acid (HF). The nanometric finger electrodes ($W_{el} = 140 - 300$ nm) were lithographically defined via electron-beam lithography. Then, 60 nm of aluminum were evaporated and the features were lifted off in Microposit Remover 1165 at 85°C. Later, lift-off of sputtered Al was employed to define the probing pads. This step is optional, and was performed to ease the e-beam lithography process. In a foundry, where cost-effectiveness and throughput are prioritized, those two steps could be merged employing a deep-UV stepper lithography tool. Finally, XeF_2 isotropic etching was performed to release the devices (Fig.3). The testing was performed via direct probing with two Cascade GS150 RF probes. The devices scattering parameters were recorded employing a Keysight N5221A network analyzer.

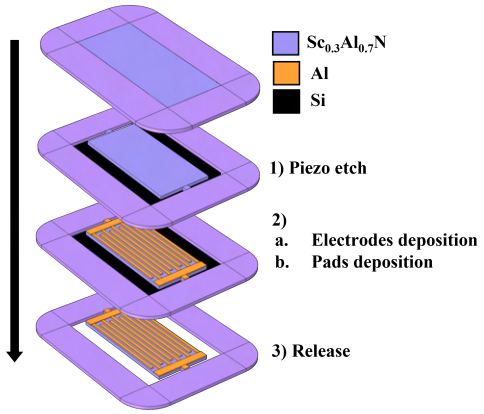

Figure 3: Micro-machining process employed to fabricate the devices of this work.

Standalone resonators

Standalone CLMRs operating in the 7-11.1 GHz range were measured, showing a wide on-chip lithographic tunability of the resonance frequency without major degradation of the k_t^2. In particular, setting 9.05 GHz as center frequency, a band of $\pm 22.5\%$ can be covered. The admittance response of six showcase devices is shown in Fig.4a. Their 3dB quality factor ($Q_{3dB} = f_s/BW_{3dB}$) and the single mode coupling ($k_t^2 = k_{tSM}^2 = \pi^2/8(f_p^2 - f_s^2)/f_s^2$, f_p being the anti-resonance frequency) are reported in Table 1, along with a comparison with CLMRs operating above 5 GHz from other works ([8][10]). Although the devices design was optimized via Finite Element Modeling (FEM) simulation employing COMSOL® Multiphysics, *a-posteriori* simulations taking into consideration the actual fabricated geometrical dimensions were carried out to verify the results agreement. The 2D simulation outputs in terms of resonance frequency are reported in Fig.4b,

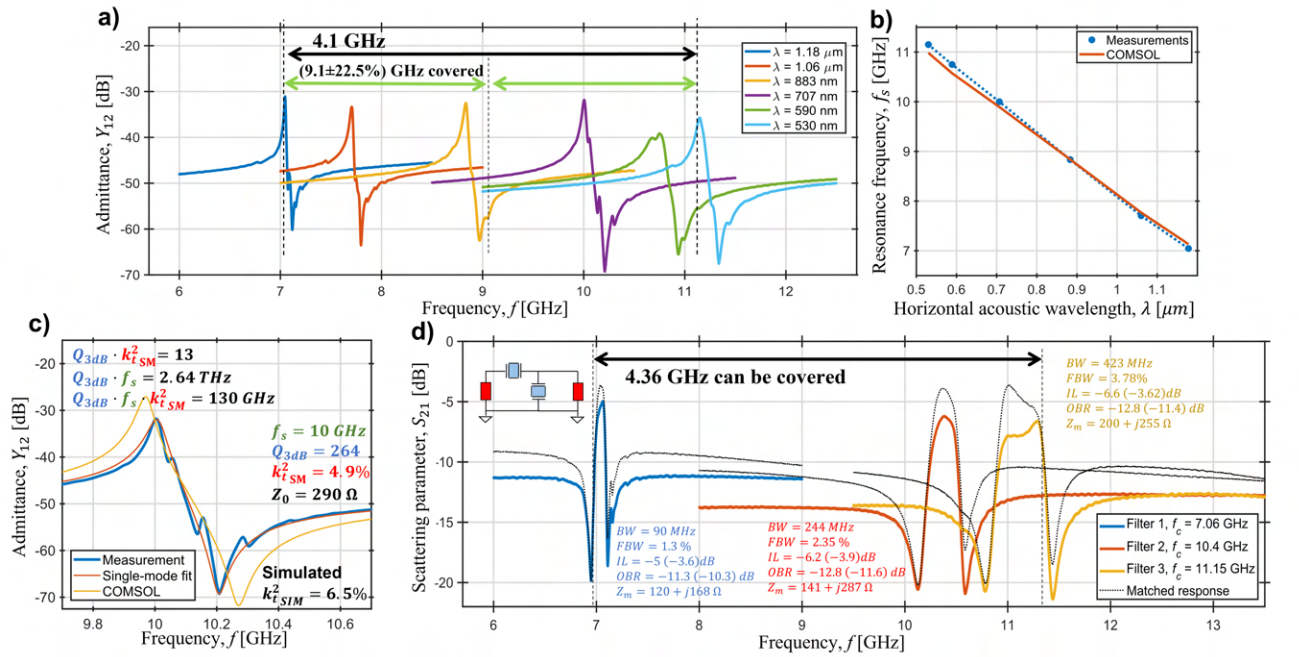

Figure 4: a) High-performance SHF CLMRs, showing the wide 4.1 GHz range covered by devices fabricated on the same chip. The resonators Q and k_t^2, along with the relative FoMs, are reported in Table 1. b) agreement of FEM simulation with the experimental results in predicting the resonance frequency (relative error < 2.5%). c) Zoom-in on the best resonator of this work, along with its single-mode fitting employing an mBVD model, a-posteriori COMSOL simulation, main metrics and figures of merit. In the simulation, the mechanical quality factor was set equal to the measured one. d) S_{21} scattering parameters of three of the fabricated filters. The frequency span and the main filter metrics are highlighted.

showing the power of predictability via FEM simulation (f_s determined with a relative error < 2.5%). Moreover, the most performing resonator of this work in terms of Q and k_t^2 is shown in Fig.4c, along with its single-mode fitting, COMSOL® simulation, and groundbreaking $f_s \cdot Q$, $Q \cdot k_t^2$ and $Q \cdot f_s \cdot k_t^2$ FoM. From Table 1, it is possible to observe how the resonators of Fig.4a follow the same simulated trends of [5] in the k_t^2 with respect to the geometrical ratio of piezoelectric film thickness and horizontal acoustic wavelength (h/λ). The ScAlN active layer, not present in the COMSOL library, was then modeled in its mechanical and piezoelectric behaviour via *ab-initio* equations derived from the density-functional theory (DFT) [4]. The employed dielectric constant, instead, was experimentally extracted utilizing an aixACCT TF 2000 thin-film characterization tool with a procedure similar to the one of [11], and found to be $\epsilon_r = 17$, higher than the DFT-predicted one of 14.

It is worth noting that, to the authors' knowledge, the $f_s \cdot Q_{3dB}$ product FoMs of all the resonators in Fig.4a besides the $\lambda = 590nm$ one are the highest ever reported on a ScAlN-based device. Moreover, their $k_t^2 \cdot Q_{3dB}$ product FoM are among the highest ever reported on an AlN-based Lamb wave resonator operating above 5 GHz (Table 1). In particular, the resonators with $\lambda = 1.18, \lambda = 883nm$,and $\lambda = 707nm$ are record-breaking. Furthermore, the resonators of the present work represent the highest-frequency devices employing such a high Sc concentration in the piezoelectric layer and the first ever employing a film sputtered from a compound casted target.

Ladder filters

For the first time above 5 GHz, ScAlN-based devices or/and CLMRs were arranged in the structure of first-order pass-band ladder filters. In particular, filters at 7, 10, and 11 GHz were synthesized and fabricated, taking advantage of the same lithographic tunability of the resonance frequency of the devices composing them. Therefore, no additional fabrication step was employed, showing the substantial advantage with respect to the high-performance, but less versatile FBARs. The filters S_{21} scattering parameter response is shown in Fig.4d. Their main metrics such as center frequency (f_c), bandwidth (BW), fractional bandwidth (FBW), insertion loss (IL), and out-of-band rejection (OBR) are all reported in the same figure. Very wide FBWs were obtained, culminating in the 3.78% of the presented filter at 11 GHz which represents, to the authors' knowledge, the highest ever reported in the literature above 10 GHz, when employing the microacoustic technology. For the IL, no specific design optimization was followed in this work, leaving the present paper as a first-of-a-kind demonstration of the ScAlN capabilities in the SHF range more than an engineering performance enhancement effort. In terms of OBR, the obtained values are relatively high for a first-order ladder filter. The reason relies in the static capacitance ratio of the parallel and series resonator

Resonator	Sc[%]	f_s [GHz]	Q_{3dB}	k^2_{tSM} [%]	$Q_{3dB} \cdot k^2_{tSM}$	$Q_{3dB} \cdot f_s$ [THz]	$Q_{3dB} \cdot f_s \cdot k^2_{tSM}$ [GHz]
λ = 1.18 μm	30	7.046	447	2.72	12.16	3.15	85.7
λ = 1.06 μm	30	7.705	240	2.95	7.1	1.85	54.55
λ = 883 nm	30	8.834	219	3.9	8.54	1.934	75.45
λ = 707 nm	30	10	264	4.9	12.93	2.64	129.4
λ = 590 nm	30	10.77	60	4.29	2.57	0.65	27.72
λ = 530 nm	30	11.15	167	4.22	7.05	1.84	78.6
Res. from [10]	0	11	615	1.3	8	6.765	88
Res. from [8]	12	8.95	5*	5.01	0.25	0.0447	2.24

Table 1: Showcase of the resonators presented in this work, along with their ground-breaking Figures of Merit. Moreover, the designs are compared with the two main works showing CLMRs above 5 GHz, showing once more the novelty of the presented devices in terms of main metrics and technological figures of merit.
$*$The paper did not report the Q_{3dB}, nor the presented admittance (Fig. 7d of [8]) showed any. Therefore, it was extracted interpolating the curve outside the limit of the X-axis.

composing it, designed to be equal to 4. This resulted in an overall increase of the IL given the lower performance of the parallel resonator. Future research efforts will include filters with a smaller capacitance ratio, together with higher order ones to combine low IL and high OBR. Finally, as shown in Fig.4d, the filters were matched to higher impedances compared to the 50 Ω of the network analyzer. This has been done employing Advanced Design System (ADS) simulations, and was carried out in order to remove the return losses from the equation and consider only the losses coming from the physical limitation of the resonator performance. The IL and OBR values in parenthesis in the insets of Fig. 4d are referred to the post-processed data.

III. CONCLUSIONS

The present work demonstrated, for the first time, the outstanding capabilities of the highly-doped ScAlN platform in the framework of SHF microacoustic devices. In particular, by leveraging the deposition of high-quality ScAlN thin-films and the optimized design and micro-machining process, record-breaking resonators were fabricated and tested in an almost unexplored frequency range, showing wide on-chip tunability. Moreover, the same resonators have been arranged in the structure of first-order ladder filters, showcasing unprecedented fractional bandwidths. Those bleeding-edge performance are combined with the post-CMOS compatibility of ScAlN and the very simple fabrication process performed on 200 mm wafers. Therefore, the present work poses itself as necessary milestone toward a possible commercialization and mass-production of high-BW, high-performance, and compact microacoustic filtering devices for the RF front end of mobile hardware exploiting the 5G-advanced and future 6G communication protocols.

ACKNOWLEDGEMENTS

This work was supported by Raytheon Missiles and Defense under contract No. 4202341711.

REFERENCES

[1] "IEEE 5G and beyond technology roadmap white paper," 2017.

[2] G. Chen and M. Rinaldi, "Aluminum Nitride Combined Overtone Resonators for the 5G High Frequency Bands," in *IEEE Journal of Microelectromechanical Systems*, 2020.

[3] Y. Yang, R. Lu, L. Gao, and S. Gong, "10–60-ghz electromechanical resonators using thin-film lithium niobate," *IEEE Transactions on Microwave Theory and Techniques*, vol. 68, no. 12, pp. 5211–5220, 2020.

[4] M. A. Caro, S. Zhang, T. Riekkinen, M. Ylilammi, M. A. Moram, O. Lopez-Acevedo, J. Molarius, and T. Laurila, "Piezoelectric coefficients and spontaneous polarization of ScAlN," in *Journal of Physics: Condensed Matter*, vol. 27, May 2015.

[5] G. Giribaldi, L. Colombo, B. Fabio, C. Cassella, and M. Rinaldi, "Investigation on the impact of scandium-doping on the kt2 of $Sc_xAl_(1-x)N$ cross-sectional lame' mode resonators," *IEEE International Ultrasonics Symposium 2020*, 2020.

[6] C. Cassella, Y. Hui, Z. Qian, G. Hummel and M. Rinaldi, "Aluminum Nitride Cross-Sectional Lamé Mode Resonators," in *Journal of Microelectromechanical Systems*, vol. 25, pp. 275–285, April 2016.

[7] Z. A. Schaffer, G. Piazza, S. Mishin, and Y. Oshmyansky, "Super High Frequency simple process flow Cross-sectional Lamé Mode Resonators in 20% Scandium-Doped Aluminum Nitride," in *MEMS 2020*.

[8] M. Park, Z. Hao, R. Dargis, A. Clark, and A. Ansari, "Epitaxial aluminum scandium nitride super high frequency acoustic resonators," *Journal of Microelectromechanical Systems*, vol. 29, no. 4, pp. 490–498, 2020.

[9] H. Holma, H. Viswanathan, and P. Mogenses, "Extreme massive mimo for macro cell capacity boost in 5g-advanced and 6g," in *Nokia Bell Labs, White paper*, 2021.

[10] M. Assylbekova, G. Chen, G. Michetti, M. Pirro, L. Colombo, and M. Rinaldi, "11 ghz lateral-field-excited aluminum nitride cross-sectional lamé mode resonator," in *2020 Joint Conference of the IEEE International Frequency Control Symposium and International Symposium on Applications of Ferroelectrics (IFCS-ISAF)*, pp. 1–4, 2020.

[11] M. Pirro, B. Herrera, M. Assylbekova, G. Giribaldi, L. Colombo, and M. Rinaldi, "Characterization of dielectric and piezoelectric properties of ferroelectric alscn thin films," in *2021 IEEE 34th International Conference on Micro Electro Mechanical Systems (MEMS)*, pp. 646–649, 2021.

CONTACT

giribaldi.g@northeastern.edu